Surface Enrichment in a Miscible Polymer Blend: An Experimental Test of Self-Consistent Field and Long-Wavelength Approximation Models

J. Genzer,*,† A. Faldi,‡ R. Oslanec, and R. J. Composto

Department of Materials Science and Engineering and Laboratory for Research on the Structure of Matter, University of Pennsylvania, Philadelphia, Pennsylvania 19104-6272

Received July 28, 1995; Revised Manuscript Received May 9, 1996[⊗]

ABSTRACT: Neutron reflectivity (NR) and low-energy forward recoil spectrometry (LE-FRES) were used to study surface enrichment in miscible blends of deuterated polystyrene, d-PS, and poly(styrene-*co*-4-bromostyrene), $PBr_{0.049}S$, having a 0.049 mole fraction of 4-bromostyrene units. The d-PS component was found to segregate preferentially to the polymer blend/air interface, whereas no enrichment of either component was detected at the polymer blend/silicon interface. The experimental values of the surface concentration, ϕ_1, and the surface excess, z^*, of d-PS were interpreted using both the theory of Schmidt and Binder (SB) (*J. Phys. II (Paris)* **1985**, *46*, 1631) and the self-consistent field (SCF) approach of Genzer *et al.* (*Phys. Rev. E* **1994**, *50*, 2373). Although both SB and SCF models were found to be in good qualitative agreement with the experimentally measured values of ϕ_1 and z^*, we demonstrate that the latter proves to be in better quantitative agreement with the experimental results. Moreover, a comparison of the SB and SCF volume fraction profiles of d-PS revealed that the SCF model described more accurately the experimental profile. We also demonstrated that adding long-range interactions to the surface potential in the SCF model produced just minor changes in the shape of the d-PS profile near the surface.

1. Introduction

Wetting, lubrication, and weatherability are just a few examples of materials properties that are controlled by the near-surface composition of polymer coatings.[1,2] These coatings may contain several components, one of which usually enriches the surface. The macroscopic characteristics can be routinely measured by traditional techniques such as contact angle measurements. However, the engineering of surface properties of polymer coatings requires control over microscopic parameters such as polymer−surface interactions, molecular weight, *etc.* With the emergence of new depth-profiling techniques, such as neutron reflectivity, the surface composition of polymers can be measured with unprecedented resolution. Combined with theoretical models, these new experimental tools have helped polymer scientists develop a better understanding of the driving forces that control the behavior of polymers at surfaces.[3] Using low-energy forward recoil spectrometry (LE-FRES) and neutron reflectivity (NR), we have measured both the surface excess, z^*, and the surface volume fraction, ϕ_1, of the segregating species in a binary miscible polymer blend. These measurements are the first rigorous test of the widely used model of Schmidt and Binder (SB) and the self-consistent field (SCF) approach. We will show that the SCF model is in better agreement with experimental results, mainly because it does not use the long-wavelength approximation made in the SB approach.

Systematic experimental studies of the surface enrichment in miscible binary polymer blends have been in progress since the first quantitative study by Bhatia and co-workers for blends of polystyrene and poly(vinyl methyl ether).[4] To date, the most complete study was carried out by Jones and co-workers, who used FRES, NR, time-of-flight FRES (TOF-FRES), and dynamic secondary ion mass spectrometry (DSIMS) to investigate the surface enrichment in isotopic blends of high molecular weight polystyrenes, d-PS:PS.[5−8] It was demonstrated that in this system the surface is enriched by the d-PS component, which has a lower surface energy than its hydrogenated counterpart. The effect of molecular weight on the surface enrichment in d-PS:PS blends was studied by Composto *et al.* using NR[9] and Hariharan *et al.* by NR and DSIMS.[10] Hariharan *et al.*[11] as well as Budkowski *et al.*[12] also studied surface segregation as a function of film thickness.

Surface enrichment was also examined in mixtures of statistical copolymers. Norton *et al.* used NR to investigate the surface enrichment of deuterated poly(ethylenepropylene), d-PEP, in isotopic mixtures of d-PEP with its hydrogenated counterpart, PEP.[13] In addition to an isotope effect, surface segregation in statistical copolymer blends can be driven by a difference in copolymer composition. For example, Steiner and co-workers used nuclear reaction analysis (NRA) to measure surface segregation of a deuterated polyethylene and poly(ethylethylene), d-PE_yPEE_{1-y}, statistical copolymer blended with PE_zPEE_{1-z} having a different copolymer composition ($y \neq z$).[14] In this system, the component with the larger PEE content was found to segregate preferentially at the surface. NR,[15,16] DSIMS,[15] TOF-FRES,[17] and LE-FRES[16] were used to investigate surface segregation in binary mixtures of poly(styrene-*co*-acrylonitrile)'s, d-S_yAN_{1-y} and S_zAN_{1-z} where $y \neq z$. It was found that the SAN with the lower AN content segregates to the surface. Recently, mixtures of a homopolymer and a statistical copolymer were used as model systems to investigate the phenomenon of surface enrichment. Bruder and Brenn[18,19] and Gluckenbiehl *et al.*[20] studied mixtures of d-PS and poly(styrene-*co*-4-bromostyrene), PBr_xS, where x is the mole fraction of the 4-bromostyrene units, and detected that the surface region was enriched with d-PS, the lower surface energy component.

† Current address: Department of Materials Science and Engineering, Cornell University, Ithaca, NY 14853.

‡ Current address: Exxon Chemical Company, P.O. Box 5200, 5200 Bayway Drive, Baytown, TX 77522-5200.

⊗ Abstract published in *Advance ACS Abstracts,* June 15, 1996.

The theory proposed by Schmidt and Binder (SB)[21] has been extensively used to interpret surface enrichment measurements obtained in many cases by direct depth profiling techniques such as DSIMS, TOF-FRES, NRA, and FRES. Given their limited depth resolution, ranging from 100 to 800 Å, these techniques were not sensitive enough to determine the detailed shape of the volume fraction profile. Instead, resolution independent values of z^* were determined and used in the SB model to calculate the volume fraction profile. After convoluting with a Gaussian function to account for the instrumental resolution, this profile was typically found to be in good agreement with the experimental one. However, this agreement could be misleading because the convolution procedure can smear out details in the shape of the volume fraction profile.

Because of its excellent depth resolution (about 10 Å), neutron reflectivity can be used to determine the detailed shape of the volume fraction profile near the sample surface. For example, in the d-PEP:PEP system NR revealed that the d-PEP profile is much flatter near the surface than that predicted by the SB theory. A breakdown of the mean-field approximation has been proposed as an explanation for this discrepancy.[13] In contrast, NR measurements on d-PS:PBr$_{0.06}$S were found to be in good agreement with predictions by the SB model.[20] This inconsistency may be due to either deficiencies in the SB theory or NR. Problems with NR, such as ambiguity in fitting the experimental data, can be removed by complimentary measurements using a direct depth profiling technique.[22] For example, Hariharan and co-workers used both NR and DSIMS to investigate surface enrichment in d-PS:PS couples and found fair agreement between the measured polymer volume fraction profiles[10,11] and those calculated using their SCF lattice model.[23] No test of the SB approach was carried out, however.

Recently, we presented a SCF model describing surface segregation in binary polymer mixtures.[24] Using Zhao *et al.*'s data on d-PS:PS measured by DSIMS,[8] SCF calculations were found to be in excellent agreement with the measured values of z^* and ϕ_1, whereas the SB approach failed to predict simultaneously z^* and ϕ_1 for the same value of the surface excess free energy. However, a direct comparison between the experimental and calculated volume fraction profiles was not presented. In this paper, we use both NR and LE-FRES to determine the volume fraction profile and z^* of d-PS, respectively, in miscible mixtures of d-PS and PBr$_{0.049}$S. The experimental results are interpreted by applying both SB and SCF models, which are both found to be in qualitative agreement with experiments. However, the SCF approach proves to be in better quantitative agreement than the SB theory.

2. Theory

2.1. Long-Wavelength Approximation Model. The first theoretical treatments describing the thermodynamics of a binary polymer mixture placed in contact with a surface (or a wall) were pioneered by Nakanishi and Pincus[25] and later refined by Schmidt and Binder.[21] The latter approach has been widely used to interpret a variety of experimental measurements. As stressed in the original paper,[21] this approach is only valid in the long-wavelength limit, $d\phi/dx \approx 1/R_g$, where R_g is the polymer radius of gyration. It is thus applicable for systems with rather moderate concentration gradients. We further refer to this approach as the SB model. Its main results are briefly summarized in this section; interested readers are referred to the original paper and references therein.

For a mixture of two polymers, A and B, the Gibbs free energy of mixing, G, per lattice site is given by

$$G(\phi_A,\phi_B) = \frac{\phi_A}{N_A}\ln[\phi_A] + \frac{\phi_B}{N_B}\ln[\phi_B] + \chi\phi_A\phi_B \quad (1)$$

In eq 1, ϕ_k and N_k are the volume fraction and number of segments of polymer k, respectively, and χ is the Flory−Huggins interaction parameter. For a polymer mixture placed in contact with a surface the total free energy per unit area, F, is given by[21]

$$\frac{F}{k_B T} = \int_0^\infty \left[G(\phi_A,\phi_B) - \Delta\mu\phi_A + \frac{a^2}{36\phi_A\phi_B}\left(\frac{d\phi_A}{dx}\right)^2 \right] dx + F_s \quad (2)$$

where k_B is Boltzmann's constant, T is the absolute temperature, $\Delta\mu$ ($= \partial G/\partial\phi$) is the exchange chemical potential, a is the segment length of A and B monomers, x is the distance perpendicular to the surface, and F_s is the "bare" surface free energy[26] that accounts for the interactions of the mixture with the surface. An analytical solution to eq 2 is possible if a simple form of F_s is used. Usually, the segment/air interactions are assumed to be of short-range character, so that only the segments directly adjacent to the surface are affected by the presence of the surface. Assuming that the A component enriches the surface, the "bare" surface free energy is only a function of the A surface volume fraction, $\phi_{A,1}$. Minimizing the energy functional (eq 2) and accounting for appropriate boundary conditions, the volume fraction profile of polymer A can be calculated from

$$x = \frac{a}{6}\int_{\phi_{A,1}}^{\phi(x)} \frac{d\phi}{\sqrt{\{\phi_A\phi_B[G(\phi_A,\phi_B) - G(\phi_{A,\infty},\phi_{B,\infty}) - \Delta\mu[\phi_A - \phi_{A,\infty}]]\}}} \quad (3)$$

where $\phi_{k,\infty}$ is the volume fraction of k in the bulk. Similarly, the expression for the surface excess of A, z_A^*, is given by

$$z_A^* = \frac{a}{6}\int_{\phi_{A,1}}^{\phi_{A,\infty}} \frac{[\phi_A - \phi_{A,\infty}]\, d\phi}{\sqrt{\{\phi_A\phi_B[G(\phi_A,\phi_B) - G(\phi_{A,\infty},\phi_{B,\infty}) - \Delta\mu[\phi_A - \phi_{A,\infty}]]\}}} \quad (4)$$

The thermodynamic driving force for segregation of polymer A to the surface is expressed as $-dF_s/d\phi_{A,1}$ and its form, derived from eq 2, is

$$-\frac{dF_s}{d\phi_{A,1}} = \frac{a}{3}\sqrt{\frac{G(\phi_{A,1},\phi_{B,1}) - G(\phi_{A,\infty},\phi_{B,\infty}) - \Delta\mu[\phi_{A,1} - \phi_{A,\infty}]}{\phi_{A,1}\phi_{B,1}}} \quad (5)$$

Recently, solutions to eq 2 have been introduced by assuming that the interactions of the polymer blend with the surface, described by F_s, are of long-range character.[27,28] Chen *et al.*[27] reported that long-range interactions change the shape of the profile of the segregated polymer significantly, whereas Jones[28] found

just minor changes in the shape of the profile. In the latter case, these change could not be detected experimentally.

Equations 3−5 define the relationships between z_A^*, $\phi_{A,1}$, and $-dF_s/d\phi_{A,1}$. Experimentally, one can measure z_A^* and then use eq 4 to evaluate $\phi_{A,1}$. Analogously, $\phi_{A,1}$ can be measured and z_A^* is determined from eq 4. Equation 5 is then applied to calculate $-dF_s/d\phi_{A,1}$. The SB model provides an accurate description of the surface segregation only if the calculated values of z_A^* and $\phi_{A,1}$ agree with their corresponding experimental quantities. Thus, only a single value of $-dF_s/d\phi_{A,1}$ exists for both calculations. In this paper we will show that neither the SB or SCF models satisfy this condition.

2.2. Self-Consistent Field Model. The SCF model used in this paper follows the framework developed by Hong and Noolandi[29] and Shull[30−32] and has been described elsewhere.[24] The polymer system is placed onto a cubic lattice with a lattice spacing of a. As in eq 2, the depth coordinate of interest is that perpendicular to the surface (positioned at $x = 0$). The probability that the tth segment of polymer k is at a distance x from the chain end is given by the distribution function $q_k(x,t)$, which is a solution of the modified diffusion equation:[33]

$$\frac{1}{N_k}\frac{\partial q_k(x,t)}{\partial t} = \frac{a^2}{6}\frac{\partial^2 q_k(x,t)}{\partial x^2} - \frac{w_k(x)}{k_B T} q_k(x,t) \qquad (6)$$

Both polymers are under the influence of a weakly perturbing mean field, $w_k(x)$, which for polymer A is given by[29−32]

$$\frac{w_A(x)}{k_B T} = \frac{1}{N_a k_B T}[\mu_A(x) - \mu_{A,\infty}] - \frac{\ln \phi_A(x)}{N_A} - \frac{\Delta w(x)}{k_B T} - \frac{w_{A,ext}(x)}{k_B T} \qquad (7)$$

where $\mu_A(x)$ and $\mu_{A,\infty}$ are the chemical potentials of polymer A at position x and in the bulk, respectively. Using the chemical potentials derived from the Flory−Huggins free energy density, eq 7 becomes

$$N_A\frac{w_A(x)}{k_B T} = \phi_{A,\infty} - \ln \phi_{A,\infty} + \left(\frac{R_{g,A}}{R_{g,B}}\right)^2 \phi_{B,\infty} - \chi N_A[\phi_{B,\infty}^2 - \phi_B^2(x)] - \left[\phi_A(x) - \left(\frac{R_{g,A}}{R_{g,B}}\right)^2 \phi_B(x)\right] - N_A\frac{\Delta w(x)}{k_B T} - N_A\frac{w_{A,ext}(x)}{k_B T} \qquad (8)$$

The incompressibility of the mixture is enforced by introducing a term $\Delta w(x)$ given by[30−32]

$$\Delta w(x) = \zeta[1 - \sum_k \phi_k(x)] \qquad (9)$$

where ζ is proportional to the bulk compressibility of the mixture. As discussed elsewhere,[24,30] the calculated volume fraction profiles are independent of the value of ζ providing the calculation converges. In practice, the optimum value of ζ is a compromise between stability and convergence rate of the SCF calculations.

The influence of the surface on polymers A and B is introduced via the external field, $w_{A,ext}(x)$. For the case of an incompressible mixture, it is sufficient to consider only one external field potential, which is given by the difference between the surface fields acting on polymers A and B. In this model $w_{A,ext}(0)$ represents the free energy gain associated with replacing a B segment at the surface ($x = 0$) with an A segment and has the form[24,30]

$$\frac{w_{A,ext}(0)}{k_B T} = \frac{1}{a}\left[-\frac{dF_s}{d\phi_{A,1}}\right] \qquad (10a)$$

As mentioned earlier, the term $-dF_s/d\phi_{A,1}$ represents the driving force for segregation and throughout this paper is called the excess surface free energy. Equation 10a is the form of the external potential for the case of short-range interactions (SRI) between the polymers and the surface. Thus, only segments within a distance a of the surface are influenced by the external surface field. Recently, we have introduced the effects of long-range interactions in the expression of $w_{A,ext}(x)$ by including van der Waals (VDW) interactions between the polymer segments and the surface. The general form of the VDW interactions for a planar interface is $F_s(x) \sim x^{-3}$.[34] The form of the long-range interaction (LRI) external potential used in the SCF model is then

$$\frac{w_{A,ext}[x = a(i-1)]}{k_B T} = \frac{1}{a}\left[-\frac{dF_s}{d\phi_{A,1}}\right](2i-1)^{-3} \qquad (10b)$$

where i is the lattice number. As is apparent from eq 10b, for $i = 1$ the LRI external potential has the same value as that in the SRI model. In the calculations, the LRI becomes negligible usually near $i \sim 3-5$, depending on the value of $-dF_s/d\phi_{A,1}$.

Self-consistent solutions to eqs 6−10 are obtained by starting with an initial choice of $-dF_s/d\phi_{A,1}$ and an initial assumption for the volume fraction profiles, $\phi_A(x)$ and $\phi_B(x)$.[35] Using appropriate initial and boundary conditions, eq 6 is solved simultaneously for both polymers[29,30] to obtain values of $q_k(x,t)$, from which the corresponding volume fraction profiles are calculated:

$$\phi_k(x) = \frac{1}{N_k}\int_1^{N_k} q_k(x,t) q_k(x, N_k - t)\, dt \qquad (11)$$

These values of $\phi_k(x)$ serve as new input for the next calculation of the distribution functions. This process is repeated until two subsequent iterations, n and $n+1$, satisfy the following condition:

$$\max_{(x,k)} |w_k^{(n+1)}(x) - w_k^{(n)}(x)| \le 10^{-4} \qquad (12)$$

The above procedure is carried out for at least five different values of $-dF_s/d\phi_{A,1}$, which are consequently used to determine z_A^* and $\phi_{A,1}$ that span the experimental values. Plots of $-dF_s/d\phi_{A,1}$ vs z_A^* and $-dF_s/d\phi_{A,1}$ vs $\phi_{A,1}$ are then fitted to a third order polynomial to find the value(s) of $-dF_s/d\phi_{A,1}$ that best reproduces z_A^* and $\phi_{A,1}$ from the experiments. Similar to the SB approach, the SCF model provides a precise description of the surface segregation only if **both** calculated values, z_A^* and $\phi_{A,1}$, agree with their corresponding experimental quantities. Moreover, a single value of $-dF_s/d\phi_{A,1}$ should be used in the calculations if the model is successful in describing surface segregation. In this work, we will show that our experimental data do not fulfill these requirements exactly. However, the experimental data are in good agreement with the SCF model and in worse agreement with the SB approach.

3. Experimental Section

3.1. Materials and Sample Preparation. The polymers used to test surface enrichment models were deuterated

Table 1. Molecular Parameters of the d-PS:PBr$_{0.049}$S System

polymer	M^a (g/mol)	N^b	polydispersity index	$(b/V)^c$ ($\times 10^6$ Å^{-2})	source
d-PS	196 000	1749	1.03	6.515	Polymer Laboratories
PBr$_{0.049}$S	400 000[d]	3902	1.05	1.432	Pressure Chemical[d]

[a] Molecular weight. [b] Number of segments. [c] Scattering length density of the polymers. [d] Refers to the parent polystyrene.

polystyrene, d-PS, and poly(styrene-*co*-4-bromostyrene), PBr$_{0.049}$S, having 0.049 mole fraction of 4-bromostyrene. The copolymer was prepared by bromination of polystyrene using the procedure of Kambour, Bendler, and Bopp.[36,37] Size-exclusion chromatography analysis of the parent PS and PBr$_{0.049}$S showed that bromination had no effect on the molecular weight distribution of the statistical copolymer. The bromination level in PBr$_{0.049}$S was determined by elemental analysis. The polymer characteristics are given in Table 1. Polymers were dissolved in toluene, and samples were prepared by spin-coating the solutions on a silicon wafer (2 in. in diameter, 4.5 mm thick) previously etched for 10 min in a 7% v/v HF/water bath. Samples were then dried in a vacuum oven at 90 °C. The volume fractions of d-PS in the as-cast films were about 0.05, 0.15, and 0.25. The corresponding film thicknesses, t, were 2550, 2030, and 1890 Å, as determined by ellipsometry. We note that these thicknesses are about 23, 18, and 17 times the bulk radius of gyration of d-PS, and therefore, no confinement effect is expected.[12] For simplicity, we represent these samples as A, B, and C, respectively. All samples were annealed under vacuum (about 10^{-4} Torr) for 4 days at 170 °C. This temperature is above the critical temperature of the mixture. The annealing time was chosen such that an equilibrium state was achieved in all samples. This assertion is justified by the large ratios of diffusion distance to sample thickness, $2\sqrt{D\tau}/t$, which is approximately 19, 19, and 18 for samples A, B, and C, respectively. In the above expressions, τ is the diffusion time and D is the mutual diffusion coefficient calculated from the fast theory[38] using known values of the tracer diffusion coefficients for polystyrene, D^*.[39] We have assumed that the low bromination level in the PBr$_{0.049}$S does not affect significantly the value of D^*.

Neutron reflectivity (NR) was used to determine the scattering length density profiles, which in turn allowed the volume fraction profiles of both polymers to be evaluated. Following NR measurements, low-energy forward recoil spectrometry (LE-FRES) was applied to measure the surface excess of d-PS at the surface. For consistency, the NR and LE-FRES measurements were carried out on the same samples. To simplify the nomenclature, the surface and bulk volume fractions and the surface excess of d-PS are denoted as ϕ_1, ϕ_∞, and z^*, respectively.

3.2. Experimental Techniques. The NR measurements were performed at the POSY II reflectometer of the Intense Pulsed Neutron Source (IPNS) at Argonne National Laboratory in Argonne, IL.[40] The principles of NR have been described extensively elsewhere.[41] Briefly, a neutron beam with a wavelength distribution $\lambda = 5-12$ Å impinges on a sample at a well-defined glancing angle, θ (usually 0.5−3.0°). Because the scattering length, b, of deuterium is much higher than that of hydrogen, labeling one of the components with deuterium provides the contrast between the labeled and nonlabeled components. In the reflectivity measurements, the intensity of reflected neutrons contains information about the scattering length density profile (b/V) as a function of the perpendicular component of neutron momentum, $k = (2\pi/\lambda)\sin\theta$. The advantages of NR are its superb depth resolution (about 10 Å) and sensitivity to abrupt changes in (b/V) gradients. At low values of k, close to the critical value, the reflectivity is extremely sensitive to the shape of the volume fraction profile near the surface. Therefore, the near-surface volume fraction profile of the segregating species can be determined very accurately.

Due to a lack of phase information reflectivity cannot be converted directly into polymer volume fraction profiles. Usually, a (b/V) profile is assumed for which a theoretically calculated reflectivity curve, corrected for instrumental resolution, is evaluated. The trial reflectivity curve is then compared to the experimental one. In the present work, we have adopted the following strategy. To cover a wide range of k, NR measurements were recorded at two different values of θ, 0.35° and 0.80°. For the data set collected at $\theta = 0.80°$, a semiautomatic routine[42] allowed us to vary the shape of the volume fraction profile of the polymers, the thickness, the roughness at the mixture/air, σ_{air}, and mixture/silicon, σ_{Si}, interfaces, and the instrumental resolution, dk/k. We used a general form of the hyperbolic tangent function, or tanh, (for details see the Appendix) to fit the shape of the volume fraction profiles of the polymers. The tanh function has been shown to be useful for describing the concentration profile of small molecule liquids at free surfaces,[43] segregation at the polymer/solid interface,[32,44] and segregation at the polymer/air interface.[12,45] For each data set the reflectivity was calculated using a standard multilayer algorithm.[41,46] The best fit to the experimental data was then obtained using the set of input parameters that produced the lowest value of χ^2_{err}, defined as

$$\chi^2_{err} = \frac{1}{n}\sum_{i=1}^{n}\left[\frac{R_{ex,i} - R_{cal,i}}{\sigma_i}\right]^2 \qquad (13)$$

where R_{ex} and R_{cal} are the experimental and calculated reflectivities, respectively, determined for n points and σ_i is the standard deviation associated with each experimental point. This procedure was repeated for the data recorded at the lower incident beam angle, allowing only the value of dk/k to change. From the fitted (b/V) profile the volume fraction profiles of both polymers can be determined. However, due to the nature of the inverse problem this fit may not be unique. To remove the critical uncertainty of NR in determining the volume fraction profiles of polymers, it is advisable to complement the NR measurements with direct profiling techniques, such as LE-FRES.

The LE-FRES measurements were carried out on a model 5SDH Pelletron tandem accelerator (National Electrostatic Corporation, WI), interfaced with a custom-designed scattering chamber at the ion beam facility of the Laboratory for Research on the Structure of Matter at the University of Pennsylvania. The details of the method have been described elsewhere.[47] In the LE-FRES technique, a monoenergetic beam of $^4He^+$ ions with an initial energy of 2.0 MeV impinges on a sample at an angle θ with respect to the sample normal. As a result of the interactions of $^4He^+$ ions with the atoms in the sample, light nuclei such as D and H recoil from the sample and travel towards an energy barrier detector that is placed at a scattering angle of 30° with respect to the incident beam. In addition to the recoiling D and H nuclei, helium is forward scattered off the carbon and silicon atoms in the polymer film and substrate, respectively. To prevent the detection of helium ions from masking the D and H signals, a 7.5 μm thick Mylar stopper foil is placed in front of the detector. The resultant LE-FRES spectrum of recoiled yield versus detected energy is then converted to a depth profile for both D and H nuclei. By using a glancing exit geometry one increases the pathlength of the recoiled particles in the sample, thus increasing their effective stopping powers, which results in better energy and depth resolutions. The experiments were carried out at $\theta = 65°$, which gave a depth resolution of about 350 Å near the sample surface. This is about 2.3 times better than the depth resolution of conventional FRES (about 800 Å), but is still insufficient to resolve the detailed shape of the volume fraction profiles. The main advantage of LE-FRES is that it can be used to determine accurately and independent of any model the integrated excess of the segregated polymer near the

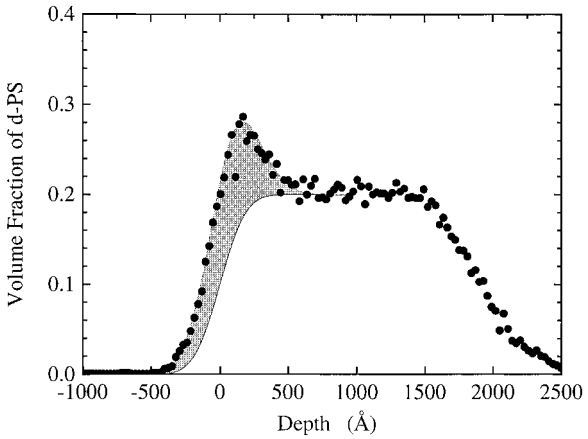

Figure 1. Volume fraction profile of d-PS as determined from the LE-FRES measurement on the d-PS:$PBr_{0.049}S$ sample annealed for 4 days at 170 °C with $\phi_\infty = 0.20$. The shaded area represents the surface excess of d-PS, z^*.

surface; thus, LE-FRES is an excellent complementary tool to NR.

4. Results and Discussion

A rigorous test of the SB, SCF-SRI, and SCF-LRI models requires measuring both z^* and ϕ_1 as accurately as possible. As mentioned earlier, LE-FRES is a particularly reliable method for measuring z^* without resorting to models. Being a direct profiling technique, LE-FRES can identify unambiguously the interface(s) being enriched. This is important because it helps to reduce the number of fitting parameters used in simulating NR results. Figure 1 shows the d-PS volume fraction profile of sample C after annealing. In agreement with previous measurements on similar systems,[18−20] the d-PS component segregates to the polymer mixture/air interface because it has a lower surface energy than its counterpart. Within the depth resolution limit of LE-FRES, the volume fraction of d-PS is uniform near the d-PS:$PBr_{0.049}S$/silicon interface, suggesting that both d-PS and $PBr_{0.049}S$ have nearly the same affinity for the silicon surface. The surface excess of d-PS is represented by the shaded region bounded by the symbols and the solid line in Figure 1. This line represents a uniform d-PS volume fraction, $\phi(x) = 0$ for $x < 0$ and $\phi(x) = 0.20$ for $x > 0$, convoluted with the instrumental resolution of 350 Å. Quantitatively, z^* is given by

$$z^* = \int_0^t [\phi(x) - \phi_\infty]\, dx \qquad (14)$$

where ϕ_∞ is the bulk volume fraction of d-PS after annealing. In a similar manner, LE-FRES was also applied to measure z^* in samples A and B.

The reflectivity data (open circles) collected from the same sample are shown in Figure 2. The upper and lower curves correspond to the reflectivities recorded at $\theta = 0.35°$ and 0.80°, respectively. The solid lines represent the reflectivities calculated from the (b/V) profiles that provided the minimum χ^2_{err}. The χ^2_{err} values were 2.06 and 1.37 for $\theta = 0.35°$ and 0.80°, respectively. The values of σ_{air} and σ_{Si} were 19 and 5 Å, respectively. The measured thickness of 1879 Å was in excellent agreement with LE-FRES and ellipsometry values. The profile shape, a truncated hyperbolic tangent function, is discussed in the Appendix.

Figure 3 shows the volume fraction profiles of d-PS for sample C determined from NR measurements (solid

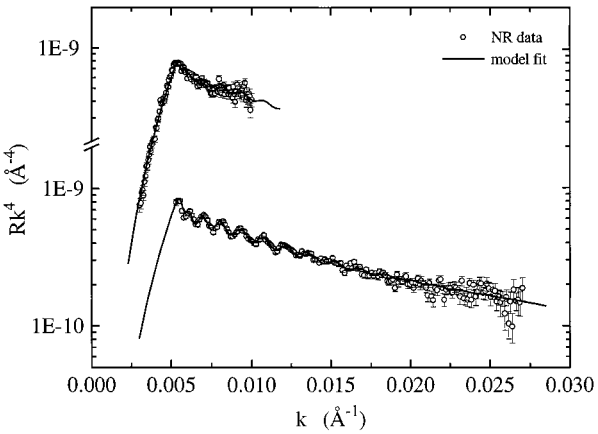

Figure 2. NR data (open circles) for the d-PS:$PBr_{0.049}S$ sample annealed for 4 days at 170 °C with $\phi_\infty = 0.20$. Data obtained at two different angles of the incident neutron beam, namely $\theta = 0.35°$ (upper curve) and $\theta = 0.80°$ (lower curve), are shown. The solid lines are the calculated reflectivities using the model volume fraction profile of d-PS shown in Figure 3.

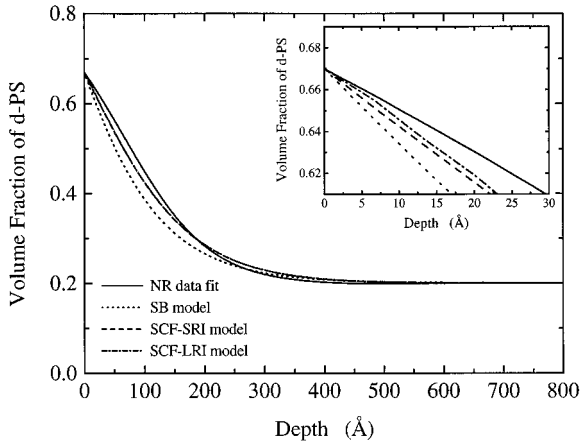

Figure 3. Volume fraction profiles of d-PS for the sample with $\phi_\infty = 0.20$, as revealed from the fit to the NR data (solid line), calculated using the theory of Schmidt and Binder (dotted line), and determined from the SCF model with the short range interaction potential (dashed line) and long range interaction potential (dash-dotted line). The inset to the figure shows the detailed shapes of the profiles in the near surface region.

line) and calculated from the SB (dotted line), SCF-SRI (dashed line), and SCF-LRI (dash-dotted line) models. We note that the reflectivity calculated from the SCF-SRI model was in poor agreement ($\chi^2_{err} = 12.55$) with the measured reflectivity. In the SB and SCF calculations, the numbers of segments of d-PS and $PBr_{0.049}S$ are given in Table 1 and χ is 7.5×10^{-4} at 170 °C. The latter value was determined by interpolating the χ's for d-PS:PBr_xS systems[48] to $x = 0.049$. In Figure 3, ϕ_1 and ϕ_∞ values of 0.67 and 0.20 are obtained directly from NR and LE-FRES measurements, respectively, and are independent of the models used to analyze either data set. For the SB model, the volume fraction profile of d-PS was calculated using eq 3. For both SCF models the values of $-dF_s/d\phi_1$ in eqs 10a and 10b were chosen such that the calculated ϕ_1 agreed with the ϕ_1 measured using NR. A comparison of the model and experimental profiles reveals that both SCF models describe the shape of the d-PS volume fraction profile in the near-surface region better than the SB approach. This observation is in accord with our previous study[24] in which the limitations of the SB model were discussed. The near-surface region of the d-PS volume fraction profile is expanded in the inset to Figure 3. This plot demon-

strates that including long-range interactions to the external potential, eq 10, does not produce major corrections to the shape of the d-PS profile in the near-surface region. We also note that we do not observe a significant flattening of the volume fraction profile of the segregated polymer in the near-surface region, a result reported by Norton and co-workers[13] for the d-PEP:PEP system and predicted in Monte Carlo simulations.[49]

The SCF profiles differ from the experimental profile for several possible reasons. First, the shape of the segregated profile is very sensitive to the value of χ, which depends strongly on x, the mole fraction of 4-bromostyrene in the poly(styrene-*co*-4-bromostyrene). Therefore, the uncertainty in determining x will result in an error.[50] Also, the value of χ used in the calculations was based on an interpolation of measured values of χ that also are associated with an error. In addition, one has to account for the effect of polydispersity in x on the phase behavior of PBr_xS. Although the thermodynamics of the PS/PBr_xS system has been widely studied,[18−20,36,48] the effect of bromination polydispersity has not yet been evaluated. However, for dilute solutions and small values of x in our study, the distribution is expected to be narrow.[51] In preliminary liquid adsorption chromatography (LAC) experiments on plain silica with hexane−tetrahydrofuran gradient, the polydispersity in bromine content of $PBr_{0.25}S$ was found to be less than the detection limit (estimated to be about 5%).[52] We thus speculate that the difference between the NR and SCF profiles is due to the uncertainty of χ. We also stress that our SCF model does not account for the non-Gaussian conformations of the chains in the near-surface region. Wijmans and co-workers used the lattice SCF model to study the effects of bond correlations and chain stiffness for polymers adsorbing onto a flat surface.[53] They found that the polymer brush thickness increases as the chain stiffness increases, whereas this thickness decreases if correlations between neighboring bonds are included. When considered simultaneously, both effects can cancel each other, resulting in a profile that is almost identical with an SCF profile calculated without these corrections. Regardless of the uncertainty of χ and the effects of chain conformations, the SCF model provides a more precise description of the shape of the segregated polymer than the SB model. In the next section the SCF and SB models will be further tested by comparing the calculated and experimental values of both z^* and ϕ_1.

Figure 4 shows how z^* measured by NR (solid circles) and LE-FRES (open circles) increases as ϕ_∞ increases. Considering that NR is relatively insensitive to the tail of the surface layer region, the agreement between the NR and LE-FRES values is excellent. At the low values of ϕ_∞ covered in this study, Figure 4 shows that the amount of the segregated polymer increases as ϕ_∞ increases. This trend in z^* correlates with that of a surface correlation length, ξ_s. At low ϕ_∞, both z^* and ξ_s increase, reach a maximum at an intermediate value of ϕ_∞, and then decrease as ϕ_∞ approaches 1, where z^* eventually goes to 0. The trends in z^* calculated by the SB (dotted line), SCF-SRI (dashed line), and SCF-LRI (dash-dotted line) models are in qualitative agreement with the variation of the measured values z^* with ϕ_∞. Although both the SB and the SCF predictions for z^* underestimate the measured values, the SB values for z^* are up to 40% lower than the experimental quantities, whereas the SCF error is only half as large. As is

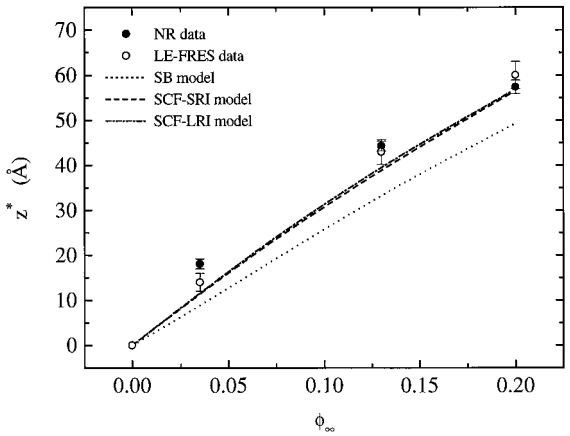

Figure 4. Variation of the surface excess of d-PS, z^*, with the volume fraction of d-PS in the bulk of the mixture, ϕ_∞. The solid and open circles are the values determined from the NR data fits and LE-FRES, respectively. Also shown are the calculation results for SB (dotted line), SCF-SRI (dashed line), and SCF-LRI (dash-dotted line) models, respectively.

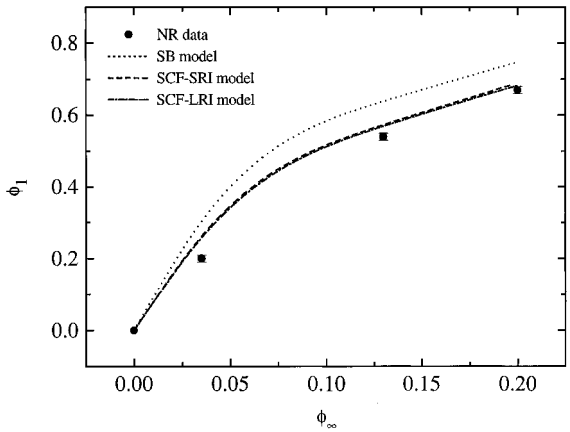

Figure 5. Variation of the surface volume fraction of d-PS, ϕ_1, with the volume fraction of d-PS in the bulk of the mixture, ϕ_∞. The solid and open circles are the values determined from the NR data fits. Also shown are the results for SB (dotted line), SCF-SRI (dashed line), and SCF-LRI (dash-dotted line) models, respectively.

apparent from the figure, accounting for possible long-range interactions improves the agreement between the SCF and experimental results only slightly. Recall that the model calculations of z^* use the values of ϕ_1 determined from NR. Conversely, the models can calculate ϕ_1 given the experimental values of z^*. Although the SB approach has been used many times to interpret experimental data, only the values of z^* or ϕ_1 were used as input parameters. In a previous publication[24] we have shown why **both** quantities must be measured if a rigorous test of surface enrichment models is to be made.

Figure 5 shows how the values of ϕ_1 determined by NR (solid circles) increase rapidly and then more slowly with increasing ϕ_∞, a trend in qualitative agreement with the SB (dotted line), SCF-SRI (dashed line), and SCF-LRI (dash-dotted line) models. Although all models overestimate ϕ_1, the SB values are up to 30% larger than the NR values whereas the SCF results are in significantly better agreement with the measured values. In both the SB and SCF models, the ϕ_1 values are based on the z^* measured by LE-FRES. Using the SCF-LRI model to predict ϕ_1 produces only a minor improvement in the agreement between the calculated and experimental values. Consistent with the discussion of

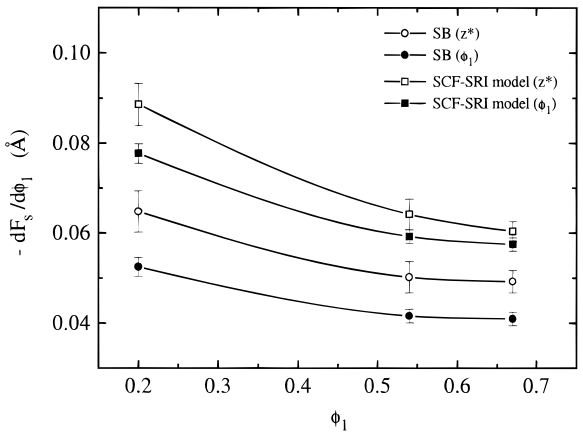

Figure 6. Variation of the excess surface free energy $-dF_s/d\phi_1$ as a function of ϕ_1 for the SB (circles) and SCF-SRI (squares) models, respectively. The open symbols represent the values calculated from the LE-FRES measurements of z^*. The solid symbols are the values determined from the NR measurements of ϕ_1. The lines are guides to the eye.

the profile shape (Figure 3), a comparison of the experimental and predicted values of both z^* and ϕ_1 demonstrates that the SCF model provides a more accurate description of surface enrichment that the SB approach. This improvement results from removing the square gradient approximation made in the SB theory.

The excess surface free energy $-dF_s/d\phi_1$ for the SB (circles) and SCF-SRI (squares) models is plotted in Figure 6 as a function of ϕ_1. In the SCF-LRI model, the values of $-dF_s/d\phi_1$ are slightly lower than the SCF-SRI values and are omitted for clarity. The solid symbols were calculated using z^* from LE-FRES, whereas the open symbols are based on ϕ_1 values determined from NR. For both models the values of $-dF_s/d\phi_1$ at a given ϕ_1 depend on the experimental data used as input parameters in the calculations. This observation suggests that both the SCF and SB models fail to predict surface enrichment quantitatively. However, at high ϕ_1, the $-dF_s/d\phi_1$ values determined from SCF are in better mutual agreement than the SB ones. This result is expected because the long-wavelength approximation is not valid when large concentration gradients are present in the system. This failure of the long-wavelength approximation occurs at the highest values of ϕ_1 covered in our experiments. We also note that the absolute magnitude of $-dF_s/d\phi_1$ is about three times larger than that reported for d-PS:PS[5,8,12,24] and approximately the same as d-PEP:PEP.[13]

Over the ϕ_1 range shown in Figure 6, $-dF_s/d\phi_1$ is a monotonically decreasing function of ϕ_1. Schmidt and Binder have proposed a simple linear dependence of $-dF_s/d\phi_1$ on ϕ_1, namely

$$-\frac{dF_s}{d\phi_A} = \mu + g\phi_1 \qquad (15)$$

which Gluckenbiehl and co-workers[20] report to be in agreement with measurements on a d-PS:$PBr_{0.06}S$ system. Recent theories have attempted to provide a more comprehensive treatment of the driving force for surface enrichment.[54,55] Particularly, the approach proposed by Cohen and Muthukumar (CM)[54] has proven to be in reasonable agreement with the nonlinear behavior of $-dF_s/d\phi_1$ vs ϕ_1 as demonstrated by recent experiments.[8] For the $-dF_s/d\phi_1$ values shown in Figure 6, we are unable to discriminate between eq 15 and the CM approach because of the limited range of ϕ_1. We can only speculate that the $-dF_s/d\phi_1$ values probably do not vary linearly with ϕ_1. Indeed, recent results on a d-PS:$PBr_{0.08}S$ system show a large deviation from linearity at large values of ϕ_1.[56]

5. Conclusion

In summary, the surface enrichment in blends of deuterated polystyrene, d-PS, and poly(styrene-*co*-4-bromostyrene), $PBr_{0.049}S$, was studied using NR and LE-FRES. After the samples were annealed, the d-PS component was found to segregate to the polymer mixture/air interface, whereas neither component enriched the polymer mixture/silicon interface. The values of the surface volume fraction, ϕ_1, and the surface excess, z^*, of d-PS were measured and the results compared with values calculated using both the Schmidt and Binder (SB) theory and the self-consistent field (SCF) approach. We have found that both the SB and SCF models provide a good qualitative description of surface segregation. However, the latter approach is in better quantitative agreement with the experimental results. For the SCF model, we have studied the effects of long-range interactions between the polymers and the surface and found that these interactions resulted in only minor changes to the shape of the d-PS profile. The SCF volume fraction profiles of d-PS, compared to the SB prediction, were in better agreement with the NR profile. However, the surface excess free energy was found to depend on whether ϕ_1 or z^* was used as input parameters in the SB and SCF models. This observation points out that caution must be used when interpreting surface enrichment experiments.

Acknowledgment. This research was supported by the Division of Materials Research, NSF Polymers Program, under Grant No. NSF-PYI-DMR91-58462, and the Monsanto Chemical Company (A.F.). The work at ANL was supported by the Division of Materials Sciences, Office of Basic Energy Sciences of the Department of Energy, under Contract No. W-31-109-ENG-38. J.G. is obliged to Professor Frans Leermakers (Wageningen University, The Netherlands) for useful discussions and advise. We thank J. Bruce Rothman for his assistance with the ion beam experiments. We gratefully acknowledge the use of the computing facilities of the Laboratory on the Structure of Matter at the University of Pennsylvania supported by the NSF MRL Program under Grant No. DMR91-20668. The ion beam facility received support from the NSF MRL Program, Grant No. DMR91-20668, the NSF Instrumentation for Materials Research, Grant No. DMR91-13697, and The University of Pennsylvania Research Facilities Development Fund.

Appendix. Functional Form of the Volume Fraction Profile Used To Simulate the NR Data

The volume fraction profile for the segregating polymer A (d-PS) used to simulate the NR data was approximated with

$$\phi_A(x) = \frac{K}{2}\left[1 - \frac{\tanh(b[x - x_{cut}])}{0.99}\right] + \phi_{A,\infty} \qquad (A1)$$

where K was given by

$$K = 2\,\frac{\phi_{A,1} - \phi_{A,\infty}}{1 - \dfrac{\tanh(-bx_{cut})}{0.99}} \qquad (A2)$$

In eqs A1 and A2 $\phi_{A,1}$ and $\phi_{A,\infty}$ were the surface and

bulk volume fractions of *A*, respectively. The parameters b and x_{cut} defined the precise shape of the profile. In particular, b (always a positive value) determined the slope of the middle part of the tanh profile, whereas x_{cut}, which ranged from $-\ln(199)/(2b)$ to $\ln(199)/(2b)$, defined the coordinate at which the tanh profile was truncated. For values of x_{cut} between $-\ln(199)/(2b)$ and 0, the profile was similar to a hyperbolic tangent, whereas for x_{cut} between 0 and $\ln(199)/(2b)$ the profile became exponential.

For a given set of $\phi_{A,1}$, $\phi_{A,\infty}$, b, and x_{cut}, the volume fraction profile of the A component was calculated using eqs A1 and A2. LE-FRES was used to determine the values of $\phi_{A,\infty}$; thus, only $\phi_{A,1}$, b, and x_{cut} were varied. Using the known volume fraction profiles and the (b/V)'s of the A and B components (listed in Table 1), the total (b/V) profile was determined from

$$\left(\frac{b}{V}\right)(x) = \left(\frac{b}{V}\right)_A \phi_A(x) + \left(\frac{b}{V}\right)_B \phi_B(x) \qquad \text{(A3)}$$

We note that in the calculations only the real components of the (b/V)'s were used; therefore, incoherent scattering from the hydrogen was not included. In eq A3 the x scale was discretized such that the "smooth" profile was converted into a histogram with an equidistant width $\Delta x = 25$ Å.[57] The (b/V) profile was corrected for roughnesses at the polymer/air (ranging between 5 and 25 Å) and polymer/silicon interfaces (ranging between 5 and 15 Å).

Registry no. provided by the author: PS, 9003-53-6.

References and Notes

(1) *Polymer Surfaces and Interfaces II*; Feast, W. J., Munro, H. S., Richards, R. W., Eds.; Wiley & Sons: Chichester, U.K., 1993.
(2) Garbassi, F.; Morra, M.; Occhiello, E. *Polymer Surfaces from Physics to Technology*; Wiley: Chichester, U.K., 1994.
(3) *Physics of Polymer Surfaces and Interfaces*; Sanchez, I. C., Ed.; Butterworth-Heineman: Boston, MA, 1992.
(4) Bhatia, Q. S.; Pan, D. H.; Koberstein, J. T. *Macromolecules* **1988**, *21*, 2166.
(5) Jones, R. A. L.; Kramer, E. J.; Rafailovich, M. H.; Sokolov, J.; Schwarz, S. A. *Phys. Rev. Lett.* **1989**, *62*, 280.
(6) Composto, R. J.; Stein, R. S.; Kramer, E. J.; Jones, R. A. L.; Mansour, A.; Karim, A.; Felcher, G. P. *Physica B* **1989**, *156, 157*, 434. Jones, R. A. L.; Norton, L. J.; Kramer, E. J.; Composto, R. J.; Stein, R. S.; Russell, T. P.; Mansour, A.; Karim, A.; Felcher, G. P.; Rafailovich, M. H.; Sokolov, J.; Zhao, X.; Schwarz, S. A. *Europhys. Lett.* **1990**, *12*, 41.
(7) Sokolov, J.; Rafailovich, M. H.; Jones, R. A. L.; Kramer, E. J. *Appl. Phys. Lett.* **1989**, *54*, 590.
(8) Zhao, X.; Zhao, W.; Sokolov, J.; Rafailovich, M. H.; Schwarz, S. A.; Wilkens, B. J.; Jones, R. A. L.; Kramer, E. J. *Macromolecules* **1991**, *24*, 5991.
(9) Composto, R. J.; Stein, R. S.; Felcher, G. P.; Mansour, A.; Karim, A. *Mat. Res. Soc. Symp. Proc.* **1990**, *166*, 485.
(10) Hariharan, A.; Kumar, S. K.; Russell, T. P. *J. Chem. Phys.* **1993**, *98*, 4163.
(11) Hariharan, A.; Kumar, S. K.; Rafailovich, M. H.; Sokolov, J.; Zheng, X.; Duong, D.; Schwarz, S. A.; Russell, T. P. *J. Chem. Phys.* **1993**, *99*, 656.
(12) Budkowski, A.; Steiner, U.; Klein, J. *J. Chem. Phys.* **1992**, *97*, 5229.
(13) Norton, L. J.; Kramer, E. J.; Bates, F. S.; Gehlsen, M. D.; Jones, R. A. L.; Karim, A.; Felcher, G. P.; Kleb, R. *Macromolecules* **1995**, *28*, 8621.
(14) Steiner, U.; Eiser, E.; Budkowski, A.; Fetters, L.; Klein, J. *Ber. Bunsenges. Phys. Chem.* **1994**, *98*, 366.
(15) Mansfield, T.; Composto, R. J.; Stein, R. S.; Rafailovich, M. H.; Sokolov, J.; Schwarz, S. A. *Physica B* **1991**, *173*, 207.
(16) Oslanec, R.; Faldi, A.; Genzer, J.; Composto, R. J. To be published.
(17) Kim, E.; Kramer, E. J.; Garrett, P. D.; Mendelson, R. A.; Wu, W. C. *Polymer* **1995**, *36*, 2427.
(18) Bruder, F.; Brenn, R. *Europhys. Lett.* **1993**, *22*, 707.
(19) Bruder, F. Ph.D. Thesis, Freiburg Universität, Freiburg, Germany, 1992.
(20) Gluckenbiehl, B.; Stamm, M.; Springer, T. *Coll. Surf. A* **1994**, *86*, 311.
(21) Schmidt, I.; Binder, K. *J. Phys. II (Paris)* **1985**, *46*, 1631.
(22) Kramer, E. J. *Physica B* **1991**, *173*, 189.
(23) Hariharan, A.; Kumar, S. K.; Russell, T. P. *Macromolecules* **1990**, *23*, 3584; **1991**, *24*, 4909; *J. Chem. Phys.* **1993**, *98*, 6516; **1993**, *99*, 4041.
(24) Genzer, J.; Faldi, A.; Composto, R. J. *Phys. Rev. E.* **1994**, *50*, 2373.
(25) Nakanishi, H.; Pincus, P. *J. Chem. Phys.* **1983**, *79*, 997.
(26) The term "bare" reflects the fact that the polymer/air interactions are assumed to be of a purely enthalpic origin.
(27) Chen, Z. Y.; Noolandi, J.; Izzo, D. *Phys. Rev. Lett.* **1991**, *66*, 727.
(28) Jones, R. A. L. *Phys. Rev. E* **1993**, *47*, 1437.
(29) Hong, K. M.; Noolandi, J. *Macromolecules* **1981**, *14*, 727.
(30) Shull, K. R.; Kramer, E. J. *Macromolecules* **1990**, *23*, 4769.
(31) Shull, K. R. *Macromolecules* **1993**, *26*, 2346.
(32) Shull, K. R. *J. Chem. Phys.* **1991**, *94*, 5723; *Macromolecules* **1992**, *25*, 2122.
(33) Edwards, S. F. *Proc. Phys. Soc. London* **1965**, *85*, 613.
(34) Israelachvili, J. *Intermolecular and Surface Forces*; Academic Press: New York, NY, 1992. Safran, S. A. *Statistical Thermodynamics of Surfaces, Interfaces and Membranes*; Addison-Wesley: Reading, MA, 1994.
(35) We usually use $\phi_A(x) = \phi_{A,\infty}$ and $\phi_B(x) = \phi_{B,\infty}$ as starting point.
(36) Kambour, R. P.; Bendler, J. T.; Bopp, R. C. *Macromolecules* **1983**, *16*, 753.
(37) ^{1}H-NMR on a PBr_xS sample with x about 0.98 confirmed that during the nucleophilic substitution reaction the bromination occurs entirely at the para position of the benzene ring of the parent polystyrene.
(38) Composto, R. J.; Mayer, J. W.; Kramer, E. J.; White, D. M. *Phys. Rev. Lett.* **1986**, *57*, 1312.
(39) Green, P. F.; Palmstrøm, C. J.; Mayer, J. W.; Kramer, E. J. *Macromolecules* **1985**, *18*, 501.
(40) Felcher, G. P.; Hilleke, R. O.; Crawford, R. K.; Haumann, J.; Kleb, R.; Ostrowski, G. *Rev. Sci. Instrum.* **1987**, *58*, 609.
(41) Russell, T. P. *Mater. Sci. Rep.* **1990**, *5*, 171.
(42) Genzer, J.; Oslanec, R. Unpublished results.
(43) Rowlinson, J. S.; Widom, B. *Molecular Theory of Capillarity*; Clarendon Press: Oxford, 1989.
(44) Nicolai, T.; Clarke, C. J.; Jones, R. A. L.; Penfold, J. *Coll. Surf. A* **1994**, *86*, 155. Clarke, C. J.; Jones, R. A. L.; Edwards, J. L.; Shull, K. R.; Penfold, J. *Macromolecules* **1995**, *28*, 2042.
(45) Hariharan, A.; Kumar, S. K.; Russell, T. P. *Macromolecules* **1991**, *24*, 4909; *J. Chem. Phys.* **1993**, *98*, 6516. Kumar, S. K.; Russell, T. P.; Hariharan, A. *Chem. Eng. Sci.* **1994**, *49*, 2899. Brazhnik, P. K.; Freed, K. F.; Tang, H. *J. Chem. Phys.* **1995**, *101*, 9143.
(46) Born, M.; Wolf, E. *Principles of Optics*; Pergamon Press: Oxford, U.K., 1975.
(47) Genzer, J.; Rothman, J. B.; Composto, R. J. *Nucl. Instr. Meth. Phys. Res. B* **1994**, *86*, 345.
(48) Strobl, G. R.; Urban, G. *Coll. Polymer Sci.* **1988**, *266*, 398. Bruder, F.; Brenn, R. *Macromolecules* **1991**, *24*, 5552.
(49) Rouault, Y.; Dünweg, B.; Baschnagel, J.; Binder, K. *Polymer* **1996**, *37*, 297.
(50) The uncertainty in determining the content of Br in the poly(styrene-*co*-4-bromostyrene) is about 0.3% as reported by Quantitative Technologies, NJ.
(51) Kambour, R. Personal communication, 1995.
(52) We are obliged to Dr. R. Perrinaud (Elf Atochem and The University of Pennsylvania) for performing the LAC analysis.
(53) Wijmans, C. M.; Leermakers, F. A. M.; Fleer, G. J. *J. Chem. Phys.* **1994**, *101*, 8214.
(54) Cohen, S. M.; Muthukumar, M. *J. Chem. Phys.* **1989**, *90*, 5749.
(55) Jerry, R. A.; Nauman, E. B. *J. Coll. Interface Sci.* **1992**, *154*, 122; *J. Chem. Phys.* **1992**, *97*, 7829; *Phys. Lett. A* **1992**, *167*, 198; *Phys. Rev. E* **1993**, *48*, 1583.
(56) Genzer, J.; Composto, R. J. Submitted for publication.
(57) Empirically we found that the reflectivity curves calculated for slab thicknesses ranging from 20 to 40 Å were identical.

MA951108F